# RSC Advances



This is an *Accepted Manuscript*, which has been through the Royal Society of Chemistry peer review process and has been accepted for publication.

Accepted Manuscripts are published online shortly after acceptance, before technical editing, formatting and proof reading. Using this free service, authors can make their results available to the community, in citable form, before we publish the edited article. This Accepted Manuscript will be replaced by the edited, formatted and paginated article as soon as this is available.

You can find more information about *Accepted Manuscripts* in the **Information for Authors**.

Please note that technical editing may introduce minor changes to the text and/or graphics, which may alter content. The journal's standard <u>Terms & Conditions</u> and the <u>Ethical guidelines</u> still apply. In no event shall the Royal Society of Chemistry be held responsible for any errors or omissions in this *Accepted Manuscript* or any consequences arising from the use of any information it contains.





# **RSC Advances**

# COMMUNICATION

# Temperature-induced work function changes in Mn<sub>1.56</sub>Co<sub>0.96</sub>Ni<sub>0.48</sub>O<sub>4</sub> thin films

Received 00th January 20xx, Accepted 00th January 20xx

DOI: 10.1039/x0xx00000x

www.rsc.org/advances

Chao Ma, ab Lei Wang, aw Wei Ren, aw Heyong Wang, ab Jinbao Xu, Jianmin Luo, abc Liang Bian, and Aimin Chang

The variations of work functions in  $Mn_{1.56}Co_{0.96}Ni_{0.48}O_4$  (MCN) thin films are investigated in the temperature range from 30 to 80 °C. The high resolution images of the contact potential difference (CPD) of MCN thin films were obtained through the Kelvin probe force microscope (KPFM) and the correlations between the work functions and temperatures were demonstrated through the imaginary part of the dielectric functions. The complex dielectric spectra are temperature dependent while their intensities have the inverse trend according to work functions. The phenomenon can be interpreted by different chemical states that relate to the  $Mn^{3+}$ .

oxides. However little is known about the effects of the ambient temperatures on the work functions of this material. Therefore, it is necessary to explore the effect of the ambient temperature on the work function of MCN film in order to design and control the electrical properties of MCN film for further applications.

been widely used in above mentioned applications since it

responses different resistance in the varying temperatures. It

is particularly suitable for the investigation of the correlation between its electrical properties and temperature <sup>6</sup>. The work

function of MCN film is an important property of the spinel

### Introduction

Transition metal oxides have attracted broad attention due to their rich physical phenomena such as metal-insulator transition, spin glass, high-temperature superconducting, and colossal magnetoresistance  $^{1,\ 2}.$  These varied electrical and magnetic properties arise from the complex interaction among spin, charge, lattice, and orbit. Because of these unique properties, spinel oxides have found potential applications in electronic, optoelectronic, and spintronic devices. Manganese cobalt nickel oxide Mn-Co-Ni-O is one of typical spinel oxide materials with large negative temperature coefficient and widely utilized as temperature compensation devices, temperature sensor devices, surge protection devices, infrared detecting bolometer and so on  $^{3,\ 4}.$  Mn<sub>1.56</sub>Co<sub>0.96</sub>Ni<sub>0.48</sub>O<sub>4</sub> is the one with a specific composition, which has the minimum resistivity compared with the other Mn-Co-Ni-O oxides  $^5.$  It has

#### **Results and discussion**

Figure 1 (a) shows the X-ray diffraction (XRD) pattern of MCN thin films deposited on Si substrates. There are six orientation peaks observed: (220), (311), (400), (422), (511) and (440). All of the diffraction peaks are identified as those from the spinel structure with the space group of Fd3m. The multi-orientation peaks indicate that the MCN spinel oxide films is polycrystalline structured. Among these peaks, the (311) peak has the strongest intensity, indicating that the (311) orientation is preferred during the film growth. Figure 1(b) illustrates the surface morphology of MCN thin films within an area of  $5\times5~\mu m^2$  at 30 °C by atomic force microscope (AFM) measurement. The film morphology is not smooth. The surface roughness of the sample is 7.8 nm. It is composed of numerous uniform-shaped particles with an averaged diameter of 200  $^\sim$  300 nm, suggesting the island-growth mode during the film growth.

<sup>&</sup>lt;sup>a</sup>Key Laboratory of Functional Materials and Devices for Special Environments of CAS, Xinjiang Key Laboratory of Electronic Information Materials and Devices, Xinjiang Technical Institute of Physics & Chemistry, Chinese Academy of Sciences, Urumqi 830011, China. E-mail: wangl@ms.xjb.ac.cn, renw@ms.xjb.ac.cn

<sup>&</sup>lt;sup>b.</sup>University of Chinese Academy of Sciences, Beijing 100049, China.

<sup>&</sup>lt;sup>c</sup>Xinjiang Uygur Autonomous Region Academy of Instrument Analysis, Urumqi 830011, China.

COMMUNICATION RSC Advances

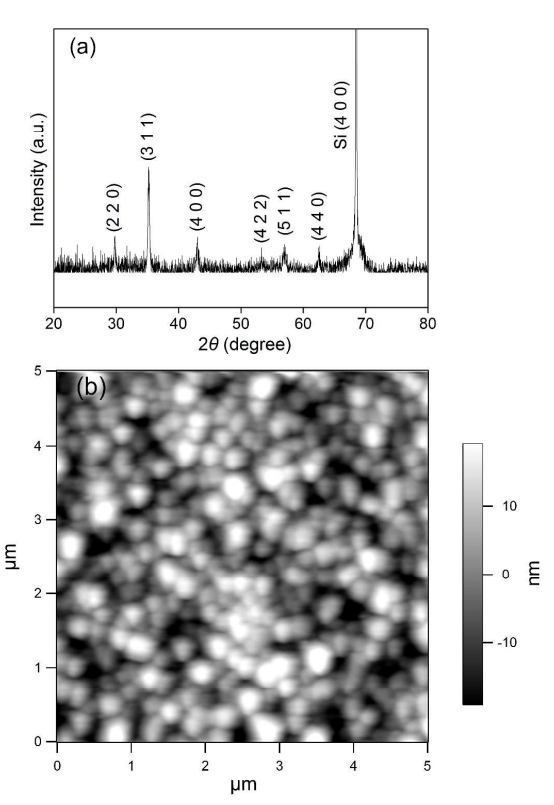


Fig. 1 (a) XRD pattern and (b) AFM image of the MCN thin films.

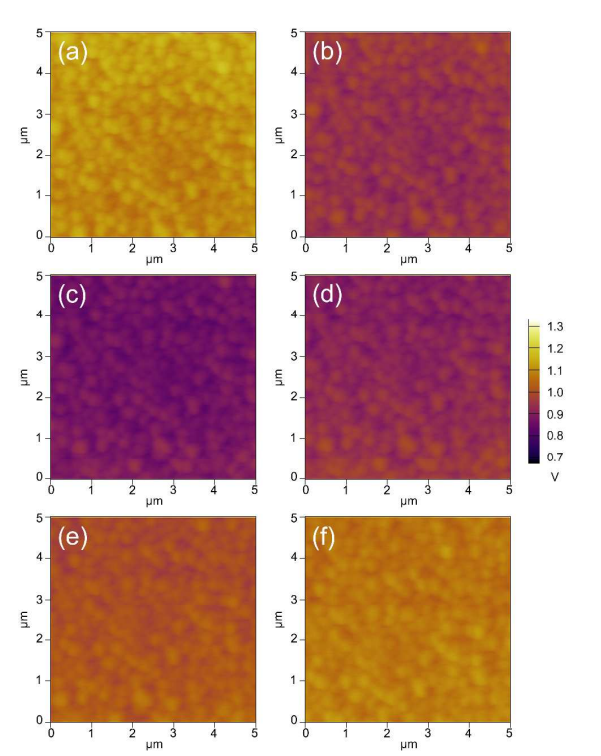


Fig. 2 The CPD of MCN thin films in the temperature of (a) 30, (b) 40, (c) 50, (d) 60, (e) 70 and (f) 80 °C respectively.

The AFM techniques exploiting electrically conducting probes have been developed to measure electrostatic forces, charge distributions, voltage drops, capacitances, or resistances. The KPFM is based on the AFM and used to measure the CPD between the AFM conductive cantilever tip and the underlying sample 7, 8. The CPD is equivalent to the surface potential voltage and can be described as the difference in the work functions between the probe tip  $(\Phi_{tip})$  and sample  $(\Phi_{sample})$ , divided by the negative electron charge (-e). Knowing the tip work function, the sample work function can be determined correspondingly (according to the equation:  $eV_{CPD} = \Phi_{tip}$  - $\Phi_{\text{sample}}$ ). In our KPFM measurement, an AC voltage is applied to the tip in order to generate oscillating electrical forces between the tip and the MCN film surface without grounding of the insulated Si substrate. Compensation of the electrostatic forces at this frequency is achieved by adjusting a DC bias to exactly match the CPD between tip and sample <sup>9</sup>. The work function of the Pt tip compared to the standard sample is 5.5 eV. The images from the AFM in figure 2 thereafter show the effects of the temperature on the CPD values of the MCN thin films. The bright and dark areas identified in these images of the MCN islands correspond to a lower and higher work function respectively. The work function is obtained by averaging the work function values over a macroscopic area of the surface. The work function values obtained through above mentioned method in each temperature are presented in figure 3. It initially increases from 4.52 eV at 30 °C, and reaches a maximum value of 4.63 eV at 50 °C, and then decrease to a minimum value of 4.43 eV at 80 °C.

Work function  $(\Phi_s)$  is regularly defined as the energy required for moving an electron from a material's Fermi level to the local vacuum level, i.e.  $\Phi_s = E_0 - E_F$ . The first term corresponds to the energy of the electrons in vacuum, and the second term is the Fermi level <sup>10</sup>. A material's work function may include two contributions: the electron chemical potential and surface dipole <sup>11, 12</sup>. The electron chemical potential represents the Fermi energy relative to the absolute vacuum level. The surface dipole represents an additional energetic barrier to removing an electron from the solid's surface <sup>13</sup>.

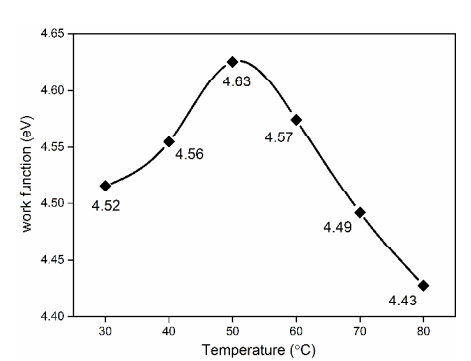


Fig. 3 The averaged work functions of MCN thin films as a function of temperature.

RSC Advances COMMUNICATION

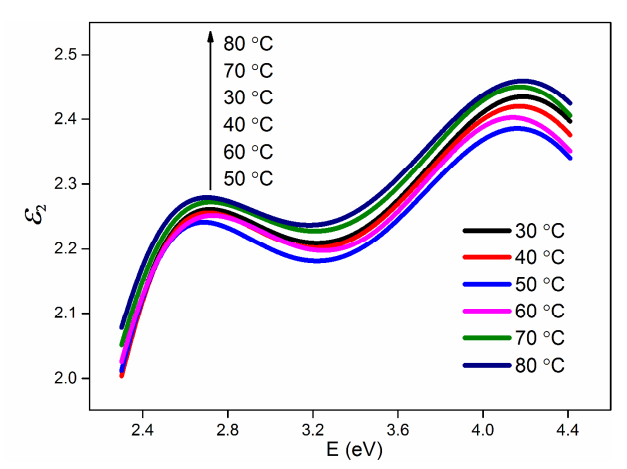


Fig. 4 Imaginary part of dielectric functions of MCN thin films under different temperatures.

In order to explore the specific variations of electrons or cations, the imaginary part of the complex dielectric function of MCN thin films were measured by spectroscopic ellipsometry (SE) at different temperatures. Considering that the imaginary part of the dielectric function reflects the interaction of electrons with a peak of maximum absorption at resonant frequency in the visible range, the electronic transitions involving different cations or their concentration can be clearly demonstrated by the imaginary part of the dielectric functions <sup>14</sup>. In our SE measurement, the TaucLorentz (TL) oscillator dispersion formula was used to model a dielectric function to represent film properties. The fourphase model (air/surface roughness layer/MCN/Si) is built to characterize the dielectric function of the films <sup>15</sup>. The TL dispersion function can be expressed as

$$\varepsilon_{2}(E) = \begin{cases} \frac{AE_{n}C(E - E_{g})^{2}}{(E^{2} - E_{n}^{2})^{2} + C^{2}E^{2}} \frac{1}{E} & (E > E_{g}) \\ 0 & (E \leq E_{g}) \end{cases}$$
(1)

Equation (1) depends on four parameters: the transition matrix element A, the peak transition energy  $E_n$ , the broadening term C, and the band gap energy  $E_g$ . All these parameters are in units of energy.

Figure 4 shows the imaginary part of the dielectric constants of MCN thin films under different temperatures. There found two broad absorption structures located at around 2.7 and 4.1 eV, respectively. The absorption structures could be related to the charge-transfer (CT) transitions involving 2p electrons of oxygen ions and 3d electrons of Mn ions, i.e.  $O^{2-}(2p) \rightarrow Mn^{3+}(3a^4)^{-16, 17}$ . The intensities of these absorption structures are related to the change of the electronic structures due to the concentration of  $Mn^{3+}$  ions<sup>16, 17</sup>. Surprisingly, we firstly found that the intensity variation trend of these SE absorption peaks with the temperature inversely matches the variation curve of the work function in figure 3. That is, the sample with the minimum absorption peak intensity (50 °C curve) has the maximum work function value and *vice versa*.

Although many factors may cause the variation of the work function, the concentration of  $Mn^{3+}$  on the topmost surface

may play an important role in our experiment. A general correlation between the cation oxidation state and the oxide's work function has been noticed. Transition metal oxides in their less-oxidized forms tend to have lower work functions compared to their higher-oxidized analogue <sup>13</sup>. And the trend is observed in our result that the increase of the lowelectronegativity cations (Mn<sup>3+</sup>) might correspond to the decrease of the high-electronegativity cations (Mn<sup>4+</sup>), which leads to the decrease of a work function. Further evidence is that AFM detect the work function values within only several topmost layers of film surface, while SE is sensitive to the film thickness of sub-atomic layer. Both techniques reflect the parameter changes of the several top atomic layers, where the oxidation/de-oxidation of Mn<sup>3+</sup> to Mn<sup>4+</sup> might be possible within a temperature range of below 80 °C. However, further detailed exploration is still needed to explain the results.

#### **Conclusions**

The polycrystalline MCN thin film has been synthesized on the Si (100) substrate. The present results demonstrate the work functions and complex dielectric functions of MCN thin films are dependent on the temperature. The varying work functions with the different temperatures in MCN thin films could be ascribed to the changes of the chemical state due to the variation of Mn<sup>3+</sup>/Mn<sup>4+</sup> content.

#### **Experimental section**

The MCN thin film was deposited on Si (100) substrates by traditional chemical solution deposition method. Mn(CH<sub>3</sub>COO)<sub>2</sub>·4H<sub>2</sub>O (AR, 99%), Co(CH<sub>3</sub>COO)<sub>2</sub>·4H<sub>2</sub>O (AR, 99%), and Ni(CH<sub>3</sub>COO)<sub>2</sub>·4H<sub>2</sub>O (AR, 99%) were selected as the raw materials with a mole ratio of Mn: Co: Ni at 13: 8: 4. These acetates were dissolved in glacial acetic acid and adjusted to 0.2 M. Then spin-coating of the solutions at 3000 rpm for 30 s was performed to form a wet film on Si substrates. Then the wet film was dried at 350 °C for 5 min. The above coating and heat-treatment procedures were repeated 10 times. The resulting films were heated at 750 °C for 1 h.

The crystal structure of the MCN thin film was investigated by XRD (with the model of Bruker D8) method. The surface morphology and work functions were investigated by AFM (Asylum Research MFP-3DTM). The imaginary part of the complex dielectric function ( $\varepsilon_2$ ) of films was obtained by SE (SENTECH SE850) with the incidence photon energy range between 2.3–4.4 eV at an incident angle of 70°. For the work function and  $\varepsilon_2$  measurement, the sample was loaded onto the heater controller module and heated from 30 to 80 °C in steps of 10 °C (with an accuracy of 0.1 °C), respectively.

#### Acknowledgments

This work was supported by the West Light Foundation of The Chinese Academy of Sciences (No. XBBS-2014-04, No. RCPY201206), the Thousand Youth Talents Plan (No.

COMMUNICATION RSC Advances

Y42H831301) and the Foundation of Director of Xinjiang Technical Institute of Physics & Chemistry, Chinese Academy of Sciences, China (Grant No. 2015RC010).

#### References

- 1. J. Chakhalian, J. Freeland, H.U. Habermeier, G. Cristiani, G. Khaliullin, M. Van Veenendaal and B. Keimer, *Science*, 2007, **318**, 1114.
- 2. A. Ramirez, R. Cava and J. Krajewski, *Nature*, 1997, **386**, 156.
- 3. M. Suzuki, J. Phys. Chem. Solids, 1980, 41, 1253.
- 4. Y. Gao, Z. Huang, Y. Hou, J. Wu, Y. Ge and J. Chu, *Appl. Phys. Lett.*, 2009, **94**, 011106.
- 5. M. Vakiv, O. Shpotyuk, O. Mrooz and I. Hadzaman, *J. Eur. Ceram. Soc.*, 2001, **21**, 1783.
- 6. J. Wu, Z. Huang, Y. Hou, Y. Gao and J. Chu, *Appl. Phys. Lett.*, 2010, **96**, 082103.
- 7. W. Melitz, J. Shen, A. C. Kummel and S. Lee, *Surf. Sci. Rep.*, 2011, **66**, 1.
- 8. J. Yang, D. Lee, K. Huh, S. Jung, J. Lee, H. Lee, D. Baek, B. Kim, D. Kim, J. Nam, G. Kim and W. Jo, *RSC Adv.*, 2015, **5**, 40719.
- 9. B. Moores, F. Hane, L. Eng and Z. Leonenko, *Ultramicroscopy*, 2010, **110**, 708.
- 10. T. Leung, C. Kao, W. Su, Y. Feng and C. Chan, *Phys. Rev. B*, 2003, **68**, 195408.
- 11. H. Ishii, K. Sugiyama, E. Ito and K. Seki, *Adv. Mater.*, 1999, **11**, 605.
- 12. K. Wandelt, Appl. Surf. Sci., 1997, 111, 1.
- 13. M. T. Greiner, L. Chai, M. G. Helander, W. M. Tang and Z. H. Lu, *Adv. Funct. Mater.*, 2012, **22**, 4557.
- 14. C. Ma, W. Ren, L. Wang, L. Bian, J. B. Xu and A. M. Chang, *Mater. Lett.*, 2015, **153**, 162.
- 15. C. Ma, H. G. Wang, P. J. Zhao, J. B. Xu, A. M. Chang, L. Wang and L. Bian, *Mater. Lett.*, 2014, **136**, 225.
- 16. W. Zhou, J. Wu, C. Ouyang, Y. Gao, X. Xu and Z. Huang, *J. Appl. Phys.*, 2014, **115**, 093512.
- 17. K. J. Kim and J. H. Lee, Solid State Commun., 2007, 141, 99.